SOCIETÀ TOSCANA DI
Scienze Naturali
RESIDENTE IN PISA

ATTI DELLA SOCIETÀ TOSCANA DI SCIENZE NATURALI

MEMORIE • SERIE A • VOLUME CXXIV • ANNO 2017

Edizioni ETS

Con il contributo del Museo di Storia Naturale dell'Università di Pisa

e della Fondazione Cassa di Risparmio di Lucca

INDICE - *CONTENTS*

Atti Soc. Tosc. Sci. Nat., Mem., Serie A, 124 (2017)
pagg. 151-169, fig. 14; *doi: 10.2424/ASTSN.M.2017.25*

Matteo Simonetti (*), Rodolfo Carosi (*), Chiara Montomoli (**)

VARISCAN SHEAR DEFORMATION IN THE ARGENTERA MASSIF: A FIELD GUIDE TO THE EXCURSION IN THE PONTEBERNARDO VALLEY (CUNEO, ITALY)

Abstract - M. Simonetti, R. Carosi, C. Montomoli, *Variscan shear deformation in the Argentera Massif: a field guide to the excursion in the Pontebernardo Valley (Cuneo, Italy).*

After a short geologic overview of the Variscan Belt in the Mediterranean Area and of the Alpine External Crystalline Massifs a field trip in the northern sector of the Argentera Massif is described. The itinerary is subdivided in six stops located along a transect that allows to observe a complete section of the Ferriere-Mollières shear zone, the main regional-scale ductile shear zone cross-cutting the Argentera Massif. This shear zone, developed at the expense of Variscan migmatites, is characterized by a deformation gradient along which a transition from protomylonites, to mylonites and to ultramylonites is welldetectable. Structural and micro-structural analysis joined with the study of kinematic vorticity allowed to recognize a transpressive deformation with variation in the percentage of pure shear and simple shear along the deformation gradient and an evolution of the shear zone from high-temperature to low-temperature conditions.

Key words - Argentera Massif, Ferriere-Mollières shear zone, mylonites, transpression, geological field trip

Riassunto - M. Simonetti, R. Carosi, C. Montomoli, *Deformazione non coassiale Varisica nel Massiccio dell'Argentera: guida all'escursione nel Vallone di Pontebernardo (Cuneo, Italia).*

Dopo un breve inquadramento geologico riguardante la Catena Varisica nell'area Mediterranea e il Massiccio dell'Argentera viene descritto un itinerario nel settore settentrionale di questo Massiccio Cristallino Esterno Alpino. Il percorso è articolato in sei *stops* lungo una trasversale completa della zona di taglio Ferriere-Mollières, la principale zona di taglio duttile che si sviluppa lungo tutto il Massiccio dell'Argentera. Questa zona di taglio, sviluppata a spese di migmatiti varisiche, è caratterizzata da un gradiente di deformazione lungo il quale è possibile osservare una transizione da protomiloniti a miloniti fino a ultramiloniti. Analisi strutturali e micro-strutturali abbinate allo studio della vorticità cinematica hanno permesso di riconoscere una deformazione di tipo transpressivo con variazioni nella percentuale di taglio puro e taglio semplice lungo il gradiente di deformazione e una evoluzione della zona di taglio a partire da condizioni di alta temperatura fino a condizioni di bassa temperatura.

Parole chiave - Massiccio dell'Argentera, zona di taglio Ferriere-Mollières, miloniti, transpressione, escursione geologica

Introduction

Shear zones separate less strained or unstrained portions of the lithosphere. They can form at all scales and at all structural levels and can record a complex polyphase deformation history (Fossen & Cavalcante, 2017 and references therein). The study of shear zones developed at the regional scale is of fundamental importance to better understand the evolution of collisional orogens because their activity can affect the P-T-t paths of the rocks involved (Carosi & Palmeri, 2002; Carosi *et al*., 2016c; Iaccarino *et al*., 2015, 2017; Kohn *et al*., 2004; Montomoli *et al*., 2013), especially for long lasting shear zones that can develop and evolve in different ways over time depending on the characteristics and the evolution of the collision (Thompson *et al*., 1997; Goscombe & Gray, 2009).
In recent years many works deal with this issue from different points of view and integrate different methodologies to obtain information about the deformation regime (Carosi & Palmeri, 2002; Law *et al*., 2004; Kurz & Northrup, 2008; Carosi *et al*., 2009) and the age and temperature of deformation (Montomoli *et al*., 2013; Iaccarino *et al*., 2015, 2017; Carosi *et al*., 2012, 2016c).
The basement of the Argentera Massif, in the Western Alps, shows beautiful expositions of folded and sheared Variscan migmatites only locally affected by Alpine tectonics. This Massif is divided in two metamorphic complexes by a 25 km long shear zone known as the Ferriere-Mollière shear zone (Malaroda *et al*., 1970; Carosi *et al*., 2016a).
The aim of the field trip is to show some key outcrops that allow to understand the evolution of the Ferriere-Mollières shear zone and the relationships between Variscan and Alpine deformation in the Argentera Massif with general implications on the deformation style of External Crystalline Massifs.

The Variscan Belt In The Mediterranean Area

The Variscan Belt is the result of a continent-continent collision between Laurentia-Baltica and Gondwana that occurred between 380 Ma and 280 Ma (Arthaud & Matte, 1977; Burg & Matte, 1978; Tollmann, 1982; Matte, 1986; Franke, 1989; Di Vincenzo *et al*., 2004).

(*) Dipartimento di Scienze della Terra, Università di Torino, Via Valperga Caluso, 35, Torino, Italy. Corresponding author, E-mail: matteo.simonetti@unito.it
(**) Dipartimento di Scienze della Terra, Università di Pisa, Via S. Maria, 53, Pisa, Italy; IGG-CNR PISA, via Moruzzi 1, Pisa, Italy

The southern sector of this belt underwent reworking during the Alpine Orogeny but, despite this, several Variscan fragments are still preserved in the Mediterranean area.
Key areas to understand the evolution of the southern European Variscan Belt are the Maures-Tanneron Massif in southern France, the Corsica-Sardinia Block and the Alpine External Crystalline Massifs (Fig. 1).
Both the Maures-Tanneron Massif and the Corsica-Sardinia Block are subdivided in two zones characterized by rocks affected by different metamorphic grade separated by transpressive shear zones (Schneider *et al.*, 2014; Oliot *et al.*, 2015; Gerbault *et al.*, 2016; Carmignani *et al.*, 1994; Carosi & Palmeri, 2002; Carosi *et al.*, 2009). In both sectors it is possible to distinguish an External Zone characterized by rocks affected by low- to medium-grade metamorphism and an Internal Zone with rocks metamorphosed under high-grade conditions. According to some authors, these two sectors had to be in continuity before the anticlockwise rotation of Corsica and Sardinia because of the opening of Mediterranean back-arc basin during Miocene time (Rollet *et al.*, 2002; Rosenbaum *et al.*, 2002; Advokaat *et al.*, 2014).
The External Crystalline Massifs (Mont Blanc, Aiguilles Rouges, Grandes Rousses, Belledonne, Pelvoux, and Argentera) recorded similar evolutions common to all Pangean Europe (von Raumer *et al.*, 2009) and are made by a high-to-medium grade metamorphic basement intruded by Permo-Carboniferous granitoids. Even though they have been involved in the Alpine Orogeny, the Alpine metamorphic overprint is very weak and usually limited to metric to decametric shear zones (Compagnoni *et al.*, 2010; Carosi *et al.*, 2016a).
Reconstruction of the southern European Variscan belt is still matter of debate because of the difficulty to correlate the different Variscan fragments in the Mediterranean area (Horner & Lowrie, 1981; Stampfli *et al.*, 2002; Rosenbaum *et al.*, 2002; Advokaat *et al.*, 2014) . Further studies about the tectono-metarmorphic evolution of the Variscan relicts are certainly needed.

Geological Setting Of The Argentera Massif

The Argentera Massif is the southernmost of the Alpine External Crystalline Massifs (Fig. 1) and it is located at the boundary between Italy and France. It is composed by two metamorphic complexes made by high-grade migmatitic gneisses (Ferrando *et al.*, 2008; Compagnoni *et al.*, 2010): the southwestern Tinèe

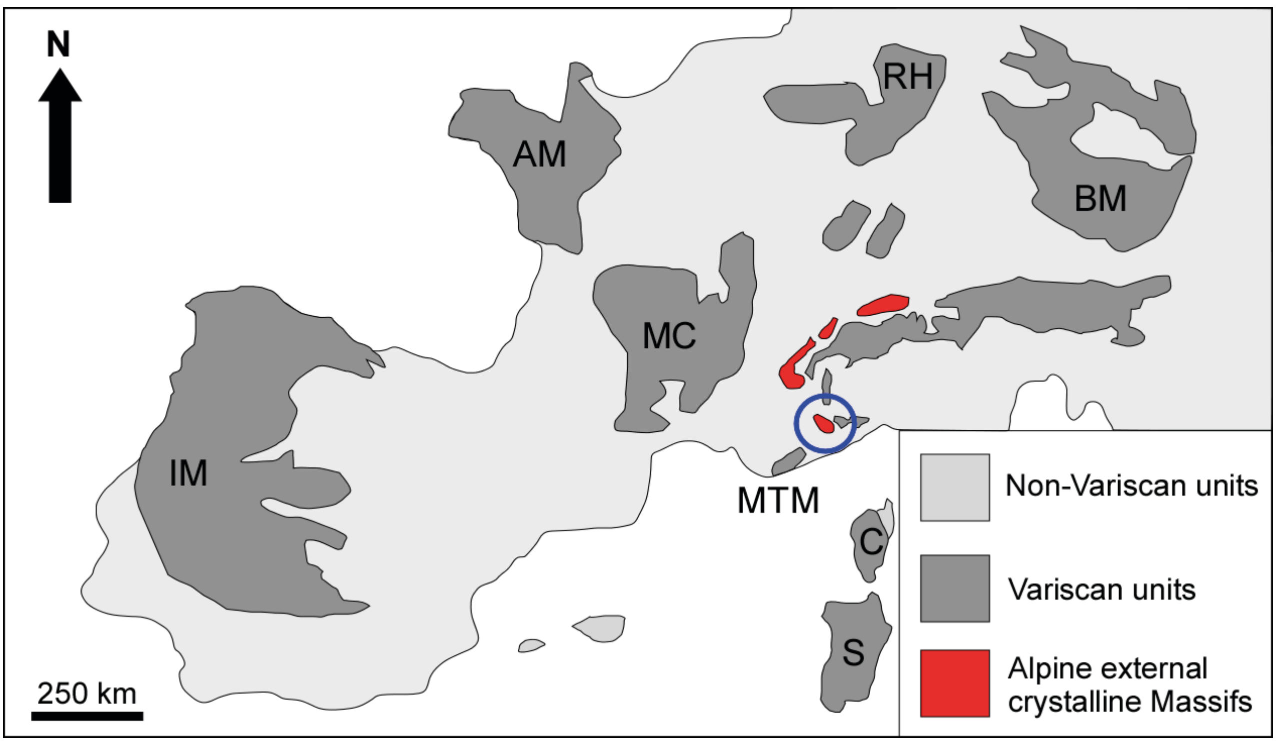

Fig. 1 - Distribution of the Variscan units in Europe at the present day. S = Sardinia; C = Corsica; MTM = Maures-Tanneron Massif; MC = Massif Central; IM = Iberian Massif; AM = Armorican Massif; RH= Rheno-Hercynian; BM = Bohemian Massif. Blue circle indicate the location of the Argentera Massif.

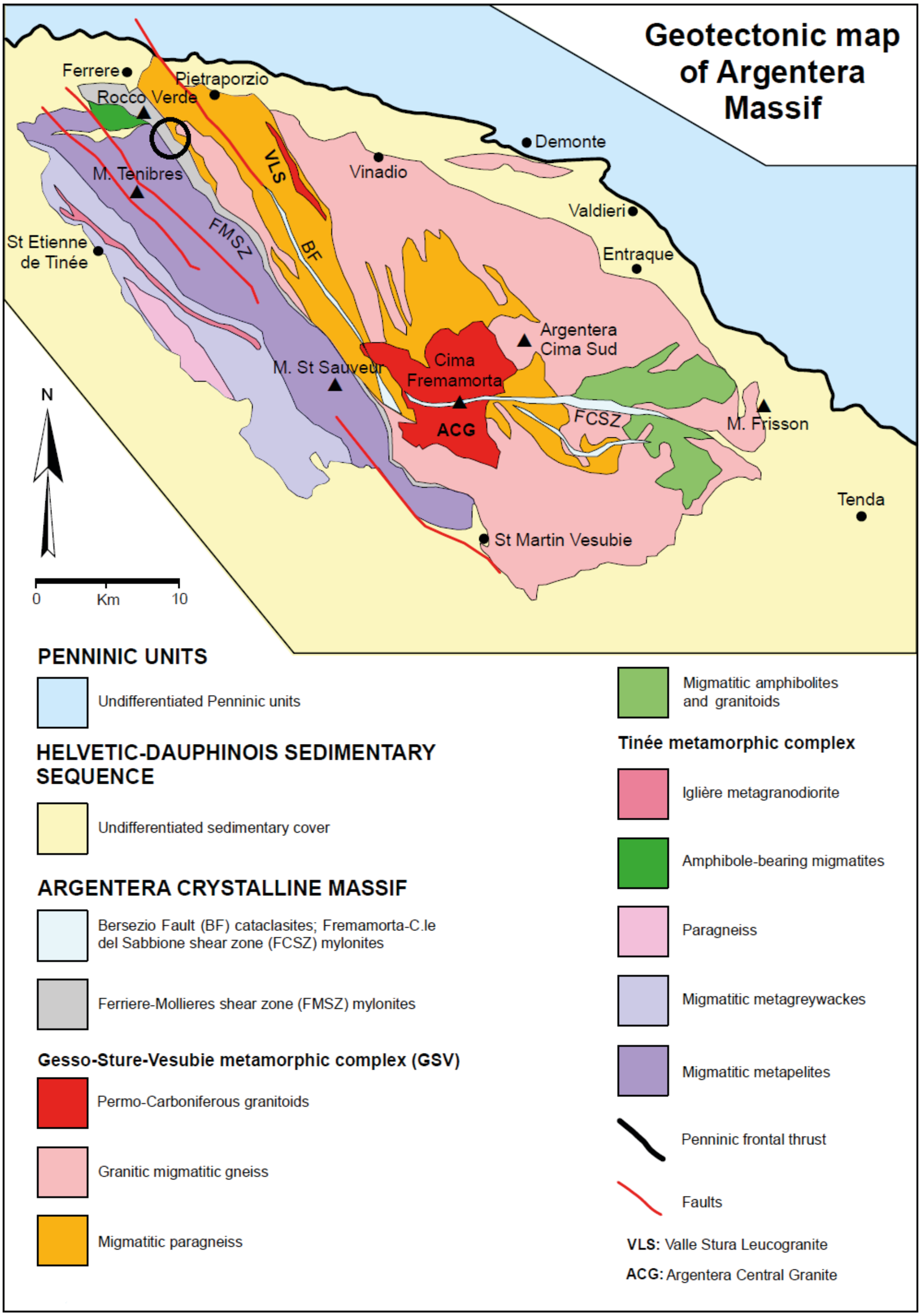

Fig. 2 - Geotectonic map of the Argentera Massif. FMSZ: Ferriere-Mollieres shear zone; FCSZ: Fremamorta-Colle del Sabbione shear zone; BF: Bersezio fault; VLS: Valle Stura Leucogranite; ACG: Argentera Central Granite (Compagnoni *et al.*, 2010). Black circle indicate the area of the field trip.

Complex and the northeastern Gesso-Stura-Vesubiè Complex (GSV), which are separated by a NW-SE striking regional shear zone, the Ferriere-Mollières Shear Zone (FMSZ) (Fig. 2).

The GSV Complex is mainly constituted by migmatitic gneiss, derived from Late Ordovician granitoids, and migmatitic paragneiss. Field relationships between the two lithotypes suggest an original intrusion of ortho-derived migmatites in the para-derived lithotypes and both types of migmatites show paragenesis indicative of amphibolite facies conditions (Compagnoni *et al.*, 2010). Associated to the ortho- and para-derived migmatites amphibolic migmatites of the Bousset-Valmasque Complex (Rubatto *et al.*, 2001), bodies of metavulcanites and mafic and ultramafic boudins are present. The study of these mafic lithotypes allowed to recognize a four stages metamorphic evolution (Rubatto *et al.*, 2010; Ferrando *et al.*, 2008; Compagnoni *et al.*, 2010): 1) HP metamorphic peak (735 ± 15° C and 1.38 ± 0.05 GPa, ~340 Ma); 2) initial decompression stage (709 ± 2° C and 1.10 ± 0.02 GPa); 3) amphibolite-facies metamorphism of HT–MP (665 ± 15° C and 0.85 GPa, ~330 Ma); 4) amphibolite-facies metamorphism of MT–LP (500 < T < 625 °C; P < 0.59 GPa, ~320 Ma). The GSV is intruded by a large granite body (Argentera Central Granite) at 292 ± 10 Ma (Rb-Sr whole rock, Ferrara & Malaroda, 1969).

The Tinée complex is divided in three "formations" (Faure-Muret, 1955) deformed under amphibolite-facies conditions: 1) Valerios-Fougieret Formation constituted by biotite and plagioclase-bearing migmatitic paragneisses with graphite and sillimanite; 2) Anelle-Valabres Formation constituted by plagioclase, biotite-bearing migmatitic metagreywakes sometimes with muscovite; 3) Rabuons Formation constituted by migmatitic metapelites, with K-feldspar, biotite, muscovite and sillimanite.

Both in Anelle-Valabres Formation and in Rabuons Formation eclogites relicts have been recognized (Faure-Muret, 1955). The Alpine greenschist-facies metamorphic overprint is generally weak and limited to shear zones cross-cutting the Variscan structures (Compagnoni *et al.*, 2010; Carosi *et al.*, 2016a).

The FMSZ is the main ductile shear zone cross cutting the Paleozoic basement of the Argentera Massif (Malaroda *et al.*, 1970; Compagnoni *et al.*, 2010; Carosi *et al.*, 2016a), it strikes NW-SE and extends from Ferriere (Valle Stura) to the northwest, to Mollières to the southeast. Recently different types of mylonites have been classified and mapped (Fig. 3) by Carosi *et al.* (2016a) according to the percentage of matrix and porphyroclasts (Sibson, 1977; Passchier & Trouw, 2005).

Across selected transects where a transition from protomylonites to mylonites and to ultramylonites has been recognized, a deformation gradient, has been detected (Fig. 4).

Methods

The northern sector of the Ferriere-Mollières shear zone has been recently mapped by Carosi *et al.* (2016a). The new structural and geological map at 1:10,000 scale covers an area of nearly 45 km^2. Mylonites have been classified according to the percentage of matrix and porphyroclasts both at the meso- and at the microscopic scale. Following Sibson (1977) and Passchier & Trouw (2005): protomylonites are characterized by 10-50% of matrix, mylonites have from 50% to 90% of matrix whereas ultramylonites have >90% of matrix.

In order to characterize the deformation regime of the Ferriere-Mollières shear zone a kinematic vorticity study was performed (Carosi et al., 2016b), using the stable porphyroclasts method (Passchier, 1987; Wallis *et al.*, 1993; Jessup *et al.*, 2007; Iacopini *et al.*, 2011) and the C' shear bands method (Kurz & Northrup, 2008; Gillam *et al.*, 2013). Selected mylonitic samples were collected in different positions within the shear zone along three transects perpendicular to the shear zone boundaries and parallel to the deformation gradient. Analyses were performed on sections parallel to the lineation and perpendicular to the mylonitic foliation (XZ section of the finite strain ellipsoid).

The study of kinematic vorticty is based on the fact that in any type of flow it is possible to recognize two lines, defined as flow apophyses (A1 and A2), along which the particles do not undergo rotation. The component of simple shear is inversely proportional to the amplitude of the angle between the two apophyses. The flow apophyses are orthogonal for pure shear flow whereas form acute angles for general shear flow and coincide for the special case of simple shear (Law *et al.*, 2004; Xypolias, 2010). The kinematic vorticity is representative of the angular speed of two orthogonal lines respect to the Instantaneous Stretching Axes (ISA, Passchier, 1991) in relation to their elongation speed. In an ISA system the non-coaxial component of the flow can be normalized to the stretching rate in order to obtain a dimensionless number that allows to compare the different types of flow. In this way it is possible to define the kinematic vorticity number as $Wk = W/|d2-d3|$ (Passchier, 1987, 1991). W represents the vorticity and d2-d3 represents the stretching rate of the principal strain axes. Wk indicates the relationship between the coaxial and non - coaxial components of the flow: pure shear is indicated by $Wk = 0$, simple shear is indicated by $Wk = 1$. Simple and pure shear contribute equally to the flow for a value of $Wk = 0.71$ because Wk is a non-linear measure (Law *et al.*, 2004; Xypolias, 2010).

Transpression and transtension are strike-slip deformations that deviate from simple shear because of a component of, respectively, shortening or extension orthogonal to the deformation zone (Dewey *et al.*, 1998).

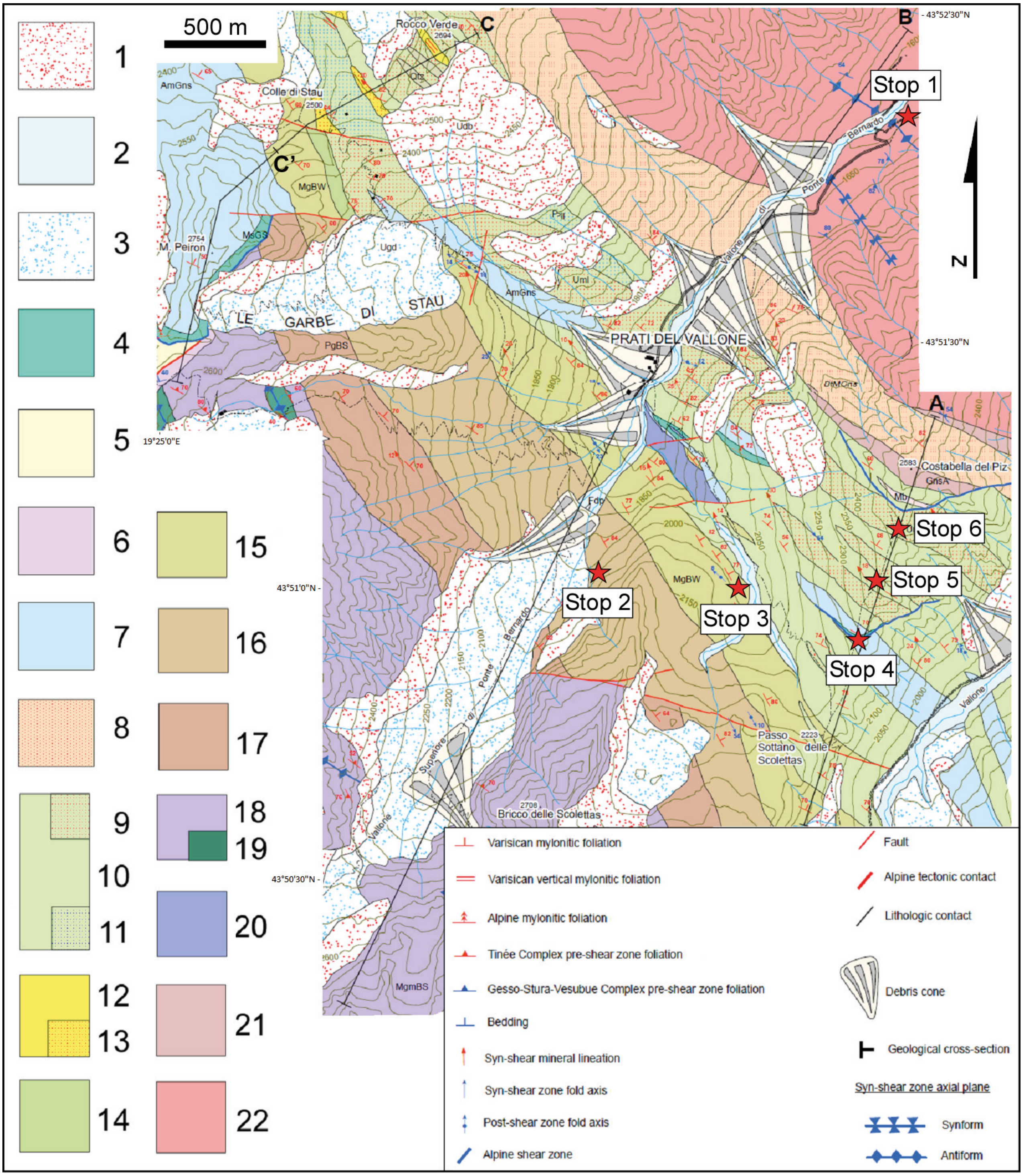

Fig. 3 - Structural-geological map of the northwestern sector of the Ferriere-Mollières shear zone at 1:10000 scale (modified after Carosi *et al.*, 2016a). 1: undifferentiated debris; 2: fluvial deposit; 3: undifferentiated glacial deposit; 4: alpine mylonitic schist with chlorite and white mica; 5: limestone breccia; 6: quarzite; 7: amphibole-bearing mylonitic gneiss; 8: biotite-bearing mylonitic gneiss; 9: ultramylonite with biotite and white mica; 10: marble; 11: mylonitic schist with biotite and white mica; 12: phyllonite; 13: mylonitic leucogranite; 14: ultramylonitic leucogranite; 15: ultramylonitic schist; 16: mylonitic gneiss with biotite and white mica; 17: mylonitic gneiss with biotite and sillimanite; 18: protomylonitic gneiss with biotite and sillimanite; 19: migmatitic gneiss with biotite and sillimanite; 20: amphibolite; 21: amphibole-bearing migmatitic gneiss; 22: migmatitic gneiss with biotite and amphibole; 23: biotite-bearing migmatite. Cross-sections A, B and C’ are reported in figure 4, figure 10c and figure 10e. Red stars show the stops of the itinerary.

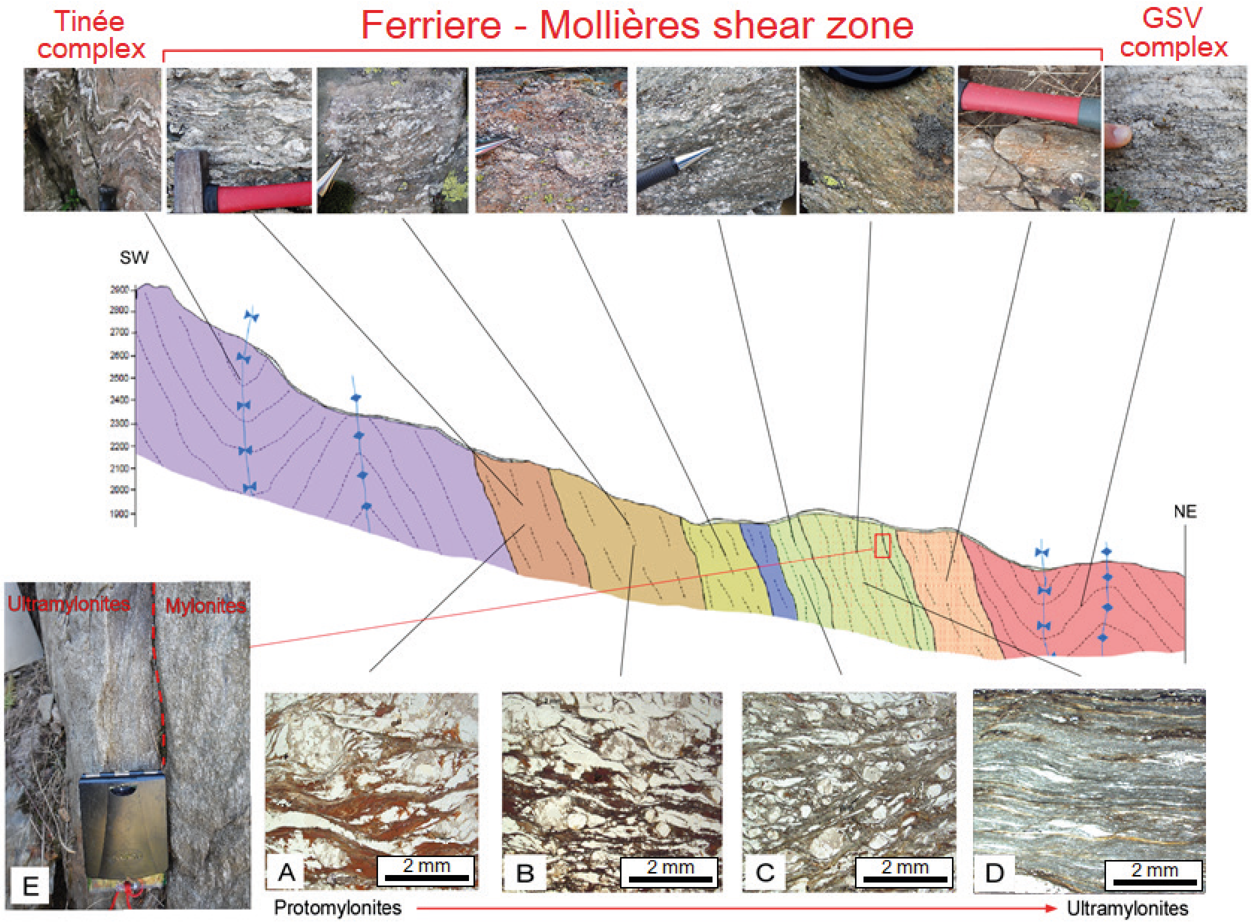

Fig. 4 - Cross-section (section B, figure 3) of the FMSZ along the Pontebernardo Valley (Carosi *et al.*, 2016a). Legend is the same as in figure 3. Tinée migmatites are represented in violet and amphibole-bearing migmatitic gneiss are represented in blue. GSV migmatites are represented in red. With the various shades of brown, green, and orange are represented the different types of mylonites belonging to FMSZ. In both the metamorphic complexes axial planes of the syn-shear zone folds are represented in blue. The transition from unsheared lithotypes of the two metamorphic complexes to the FMSZ mylonites and ultramylonites is clearly visible both at the outcrop scale and in thin section. A) protomylonites (parallel nicols); B,C): mylonites (parallel nicols); D) ultramylonites (crossed nicols); E) contact between mylonites and ultramylonites.

To distinguish between transpression and transtension, according to Fossen and Tikoff (1993) and Fossen *et al.* (1994), it is crucial to know the angles θ between the maximum Instantaneous Streching Axis (ISAmax) in the horizontal plane and the shear zone boundary. θ angles larger that 45° are indicative of transtensive deformation whereas θ angles less then 45° are indicative of transpressional deformation. The calculation, that is based on the values of the vorticity numbers obtained in the mylonites, can be made using the equation proposed by Xypolias (2010) where $W_k = \sin 2\theta$ and consequently $\theta = (\arcsin W_k)/2$.
The age of the deformation in the Ferriere-Mollières shear zone has been obtained by Simonetti (2015) and Simonetti *at al.* (2017) by LA-ICP-MS *in-situ* U-Th-Pb geochronology on syn-kinematic monazites collected in the mylonites following the procedure proposed by Montomoli *et al.* (2013 and references therein).

Geological Itinerary In The Argentera Massif

The itinerary of the field trip develops entirely in the Valle Stura di Demonte and in particular in the Vallone di Pontebernardo. This location is reachable following the road SS21 that starts from Borgo San Dalmazzo (CN) city up to the Pontebernardo village and from here following the road which leads to the locality of Prati del Vallone. Except for the transfer from stop 1 to stop 2 that is made by car, all the other transfers are possible by walking along marked trekking path (GTA path and P31 path). The whole field trip develops in a

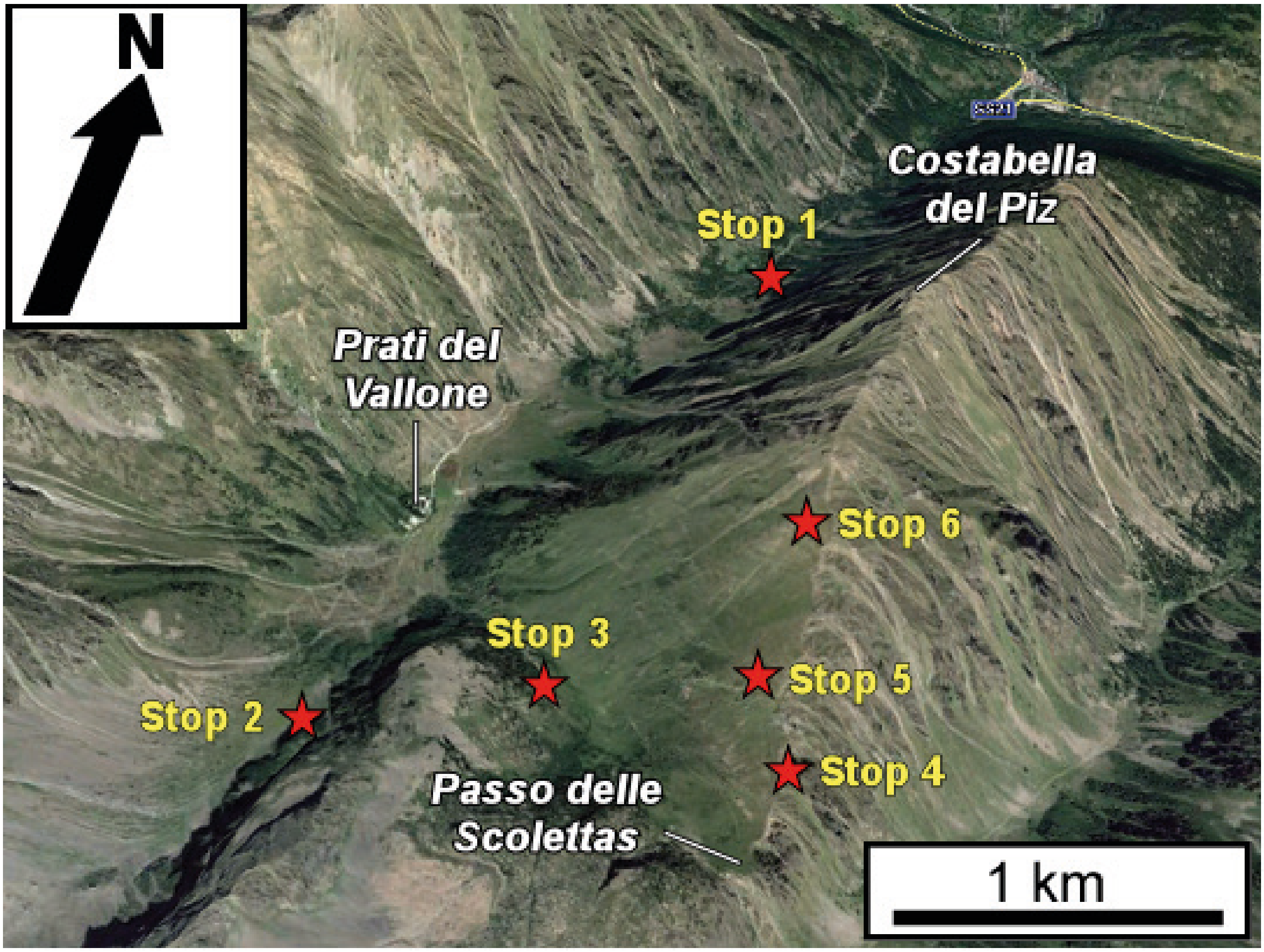

Fig. 5 - Satellite view of the Pontebernardo Valley. Red stars indicate the location of the six stops of the field trip (from Google Earth).

high mountain environment and the overall altitude difference is about 1000 m.
The itinerary is subdivided in six stops (Fig. 5) that are located along a transect that allows to observe a complete section of the Ferriere-Mollières shear zone. GPS coordinates are given in order to facilitate the finding of the outcrops.

Stop 1. Migmatites of the Gesso-Stura-Vesubie Complex (Coord. 44°20'0.87"N; 6°59'54.69"E)

From Pontebernardo we follow the road going to the locality Prati del Vallone. Halfway down the road we leave the car and follow a footpath going to a small building after few hundred metres. Here we can observe the para-derived migmatites belonging to the Gesso-Stura-Vesubie Complex (Fig. 6a).
These rocks are medium grained migmatitic gneiss with a quartz-plagioclase (An20-30)-biotite-fibrolitic sillimanite-cordierite assemblage with scarce K-feldspar and muscovite (Fig. 6b). Relict kyanite and garnet rarely included in plagioclase suggest P-T conditions of the upper amphibolite-facies (650-700°C; 0.6-0.8 GPa) and decompression from kyanite to the sillimanite stability field (Compagnoni *et al*., 1974; Compagnoni *et al*., 2010). Metric-thick leucocratic portions with less biotite locally occur. About 10-20 Ma after the Carboniferous HP metamorphism, the Argentera Massif was affected by amphibolite-facies metamorphism with extensive development of migmatites at 323 ± 12 Ma (Rubatto *et al*., 2001). Older ages for the anatectic event are reported from other Variscan migmatites in different fragments of the Variscan chain (Compagnoni *et al*., 2010; Oliot *et al*., 2015; Schneider *et al*., 2014) suggesting that several melting events may have succeeded one to each other in a complex anatectic history.
From the structural point of view the migmatite shows a gneissic foliation (Fig. 5b) that is affected by open to tight symmetric folds (Fig. 6c,d), with fold axes gently dipping toward the NW and subvertical NW-SE striking axial planes (Carosi *et al*., 2016a). A gradation-

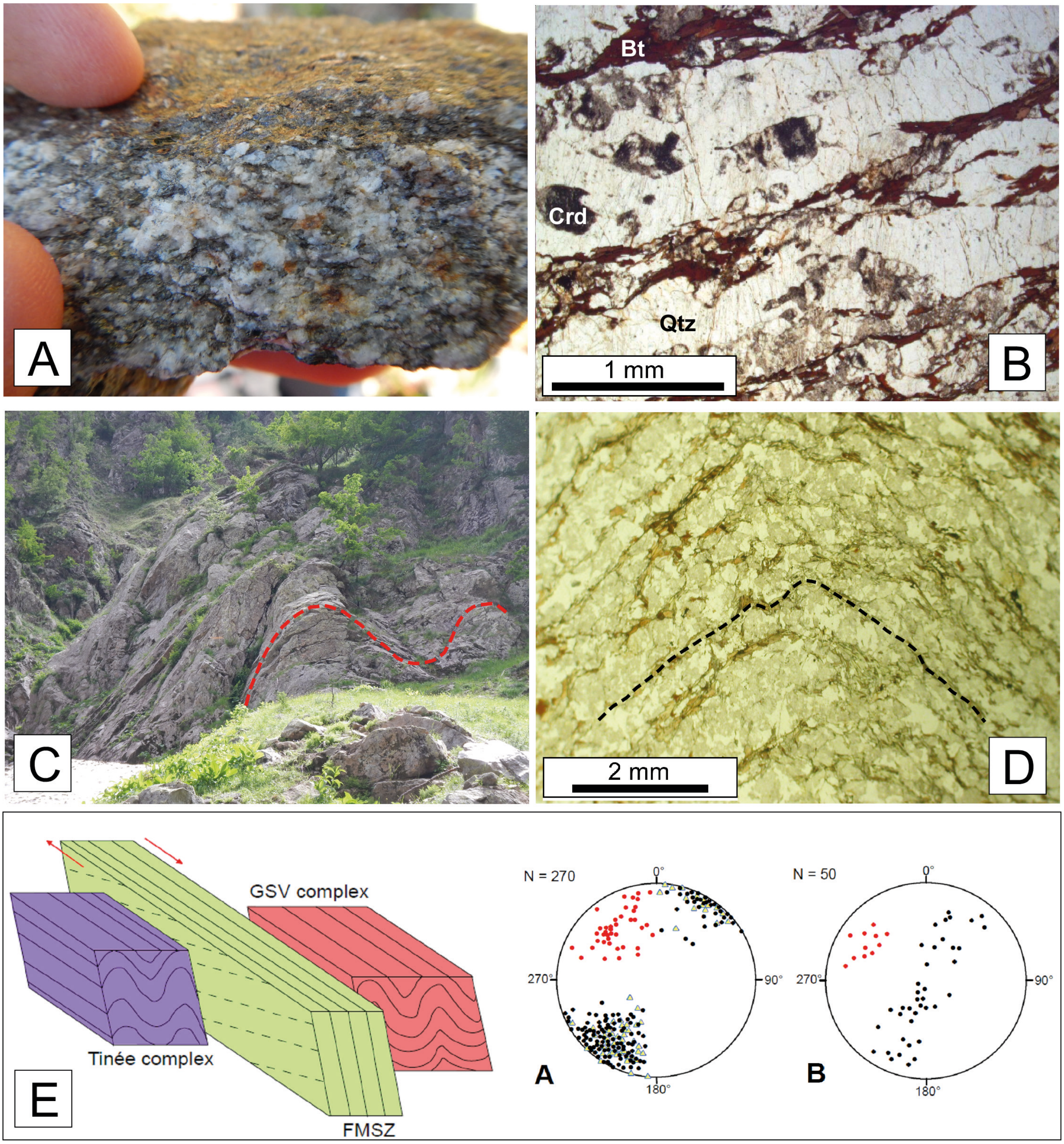

Fig. 6 - A) para-derived migmatite belonging to the Gesso-Stura-Vesubie Complex; B) alternating levels of red biotite and quartz + cordierite domains that materialize a gneissic foliation (parallel nicols); C) folds affecting the gneissic foliation of the GSV migmatites; D) gneissic foliation folded in thin section (parallel nicols); E) Relationship between the mylonitic foliation in the FMSZ and the folds observed both in the GSV and Tinée complexes, in stereonet A lineation (red dots, 40 data), poles to mylonitic foliation (black dots, 165 data) and ultramylonitic foliation (yellow triangles, 65 data) are reported, in stereonet B poles to foliation (black dots, 39 data) and fold axis (red dots, 11 data) in the Gesso-Stura-Vesubie Complex are reported (Carosi *et al.*, 2016a).

al crenulation cleavage developed parallel to the axial planes of upright folds strikes parallel to the mylonitic foliation of the FMSZ (Fig. 6e). It is possible to state that the folding event occurred in a strain regime compatible with the shearing deformation in the FMSZ and contributed to accomodate a nearly horizontal shortening (Carosi *et al*., 2016a; Carosi *et al*., 2016b).
We come back to the SS21 road and by car we reach the locality Prati del Vallone (Fig. 5) where we can leave the car. From here onwards all the stops will be reachable only by walking.

Stop 2. Protomylonites of the Ferriere-Mollières shear zone (Coord. 44°18'37.97"N; 6°58'36.11"E)
From the car park of Prati del Vallone we take the path N. P31 toward the high part of the Pontebernardo valley. On both sides of the valley protomylonite of the Ferriere-Mollières shear zone crop out (Fig. 7a).
It is possible to distinguish coarse grained protomylonitic gneiss with deformed leucosomes of K-feldspar, plagioclase and quartz in a medium grained biotite and sillimanite matrix with sometimes white mica (Fig. 7b). In some portions garnet porphyroclasts are present. The amount of matrix is variable from a maximum of nearly 50% to a minimum of 30% - 40% (Carosi *et al*., 2016a). These protomylonites developed at the expense of the para-derived migmatites of the Rabuons Formation which belongs to the Tinée Complex (Faure-Muret, 1955; Malaroda *et al*., 1970).
The main structural element in the protomylonites is a penetrative disjunctive cleavage with smooth and anastomized cleavage domain (Passchier & Trouw, 2005) rich in biotite and sillimanite (Fig. 7b) both in the prismatic and in the fibrolitic form (Carosi *et al*., 2016a). On this foliation a mineral lineation defined mainly by quartz, feldspar and subordinatly by sillimanite, is also recognizable.

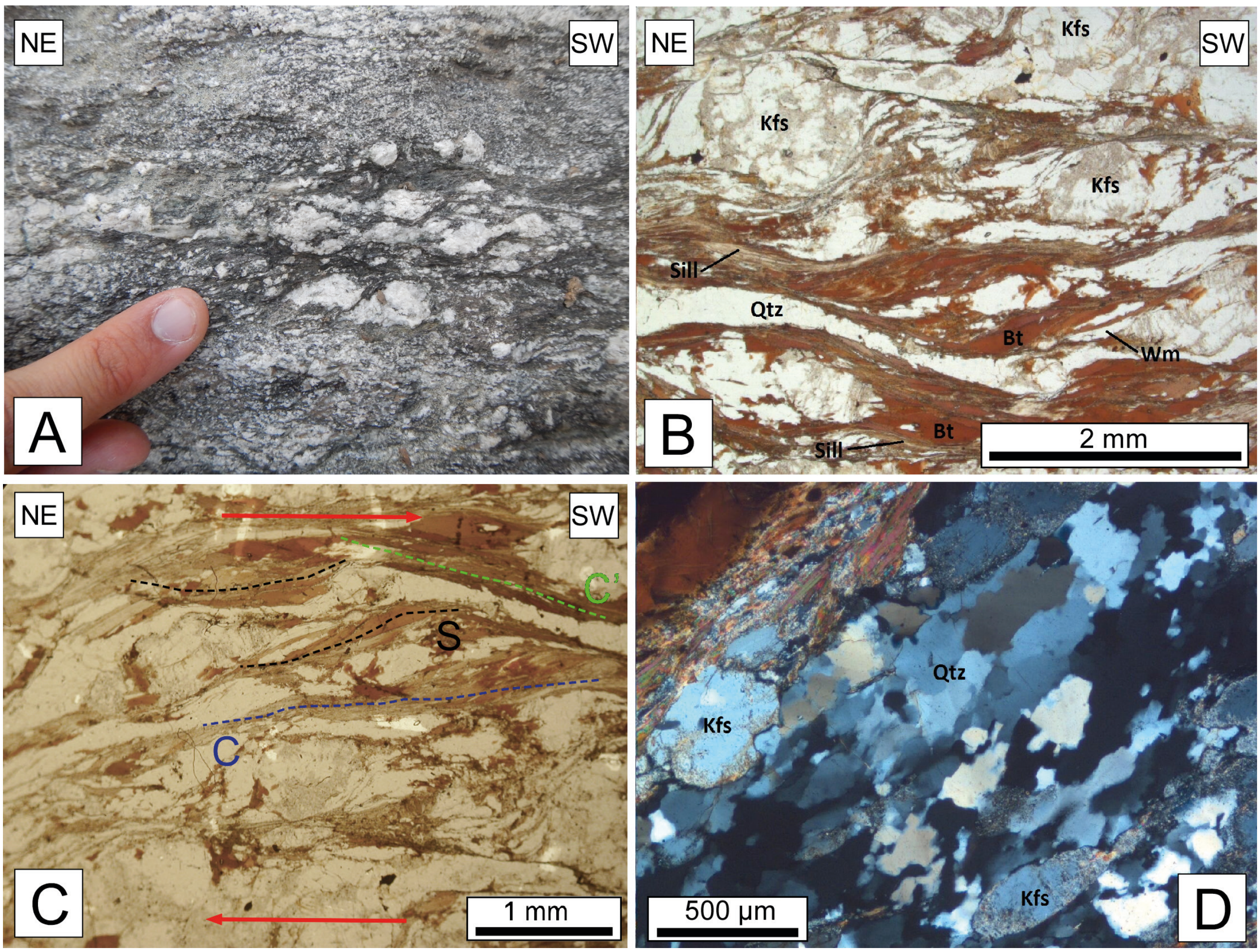

Fig. 7 - A) coarse grained protomylonitic gneiss with deformed leucosomes of K-feldspar, plagioclase and quartz in a medium grained matrix; B) protomylonite in thin section. It is possible to recognize K-feldspar, plagioclase and quartz in a medium grained biotite and sillimanite matrix with sometimes white mica; C) S-C' fabric in thin section, sense of shear is top-to-the SW; D) grain boundary migration in quartz.

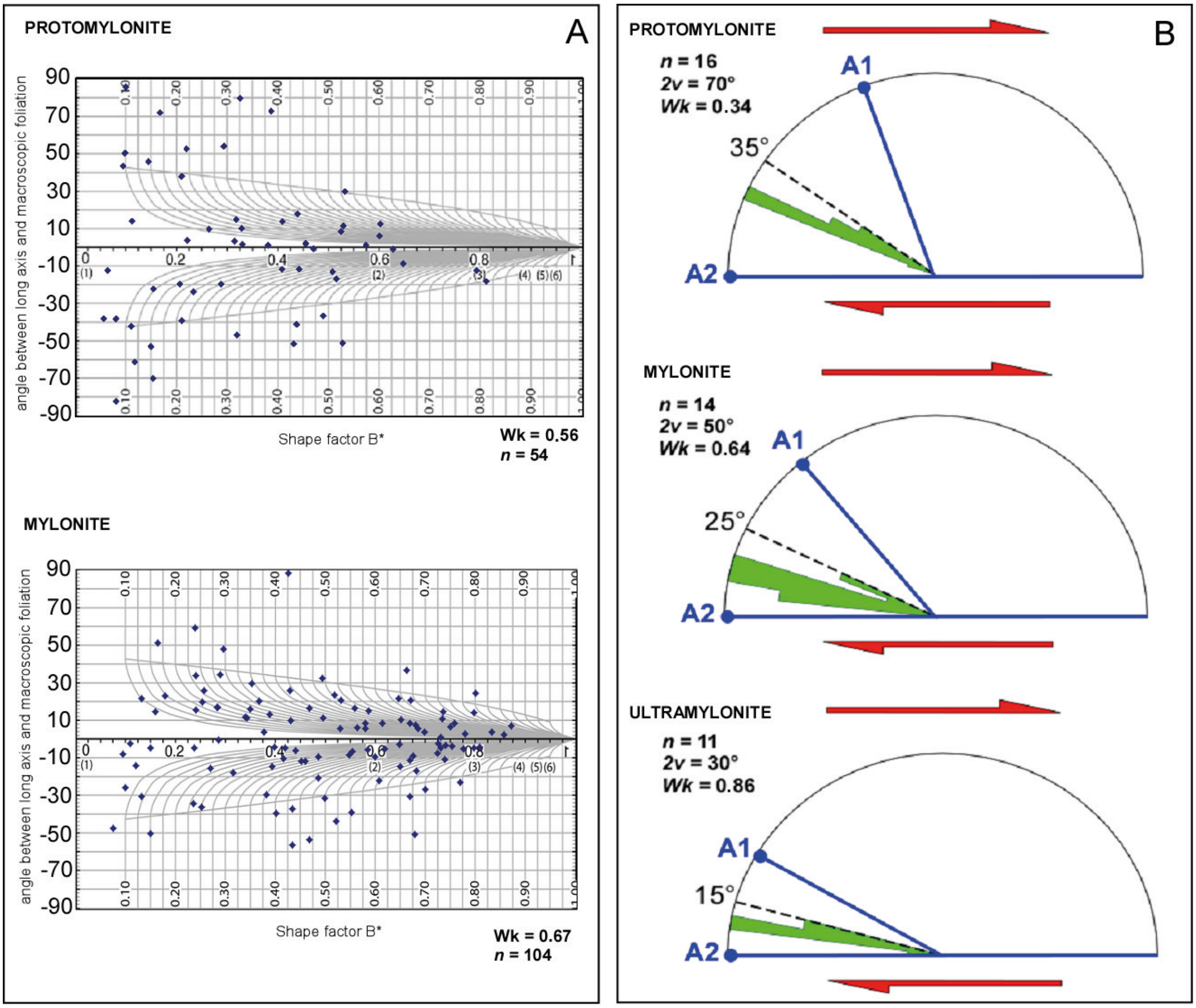

Fig. 8 - A) Kinematic vorticity analysis with stable porphyroclasts method (Passchier, 1987; Wallis *et al.*, 1993; Law *et al.*, 2004) for a protomylonitic sample and a mylonitic sample. Data are represented with Rigid Grain Net graphs (Jessup *et al.*, 2007) that show Wk values of 0.56 and 0.67 respectively for protomylonites and mylonites. These values indicate a pure shear-dominated deformation but it is possible to see an increase of the simple shear component in the mylonite; B) polar istograms used for calculating Wk with the C' shear band method (Kurz & Northrup, 2008) for a protomylonitic sample, a mylonitic sample and a ultramylonitc sample showing kinematic vorticity number (Wk) values of 0.34, 0.64 and 0.86 respectively.

Foliation strikes N100-140 and steeply dips towards both the northeast and the southwest. The mineral lineation trends N110-130 and plunge 20° towards the northwest.

At the outcrop scale S-C fabric and asimmetric and stretched leucosomes are recognizable. In thin section kinematic indicators such as porphyroclasts with asimmetric strain shadows, micafish, C' shear band and foliation fish are present. All the kinematic indicators point to a top-to-the SW sense of shear (Fig. 7c).

The presence of reddish-brown biotite and sillimanite along che C and C' planes is indicative of shear deformation during high temperature conditions. This is in agreement with the grain boundary migration (Piazolo & Passchier, 2002; Stipp *et al.*, 2002; Passchier & Trouw, 2005) deformation mecanism in quartz (Fig. 7d) (Carosi *et al.*, 2016a). Feldspars are never fractured and show undulose extinction (Simpson & De Paor, 2008) that is indicative of ductile deformation.

Recent studies about vorticity of the flow and finite strain (Carosi *et al.*, 2016b) demonstrated that these rocks developed during a deformation event dominat-

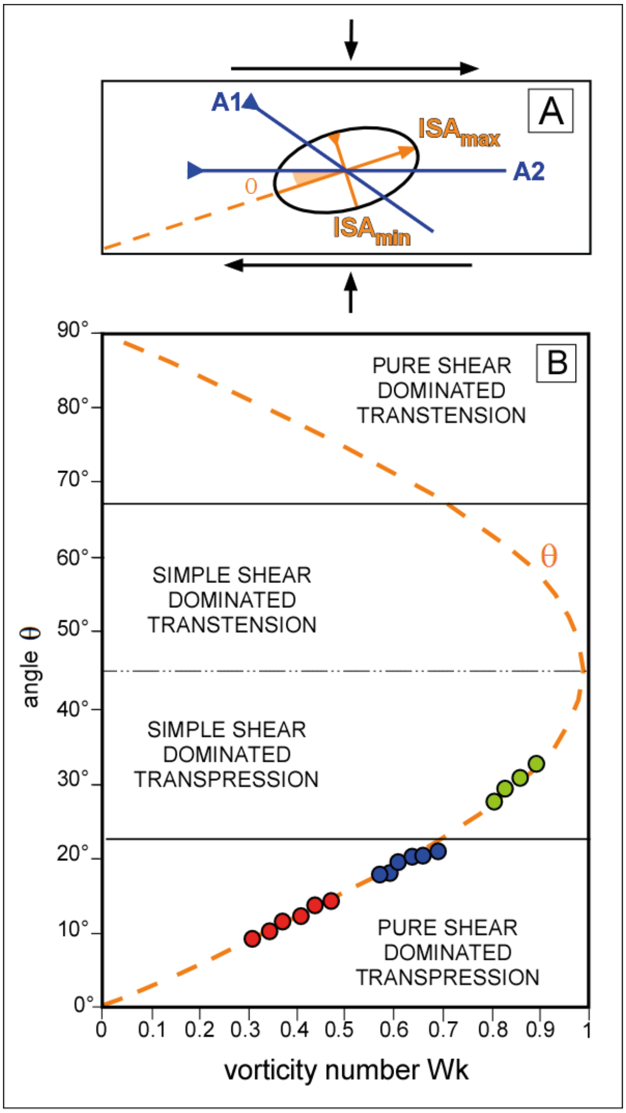

Fig. 9 - A) diagram showing relationship between the orientation of the ISAmax respect to the shear zone boundary (angle θ). A1 and A2 are the apophisys of the flow 1 and the apophysis of the flow 2 respectively; B) kinematic vorticity number Wk in relation to the calculated angle θ. Distribution of the sample clearly show a transpressive deformation with a variable component of simple shear (Carosi *et al.*, 2016b). Red circles = protomylonites, blue circles = mylonites, green circles = ultramylonites.

ed by pure shear (Fig. 8a,b). A transpressional deformation regime is confirmed by the values obtained for the angle θ (Fig. 9).
The age of shear deformation, obtained by U-Th-Pb *in situ* geochronology on syn-kinematic monazites, is ~340 Ma (Simonetti, 2015; Simonetti *et al.*, 2017).
We can now go back along the same path and take the GTA path, that starts from Prati del Vallone, toward the Passo delle Scolettas (Fig. 5).

Stop 3. Mylonitic gneiss of the Ferriere-Mollières shear zone (Coord. 44°18'50.57"N; 6°59'14.31"E)
Along the GTA path toward the Passo delle Scolettas on the left side of the small river, mylonitic migmatitic gneiss crops out in front of the Grange delle Scolettas. The mylonites present sheared leucosomes and K-feldspar, plagioclase and quartz porphyloclasts in a fine grained biotite and white mica matrix (Fig. 10a).
Garnet porphyroclasts and sillimanite relicts are present. This lithotype is very similar to the mylonitic gneiss with biotite and sillimanite, the main difference being the lower amount of sillimanite and the greater abundance of white mica. The amount of matrix in this lithotype is about 50-60% (Carosi *et al.*, 2016a).
Mineral lineation is defined by quartz and feldspar.
Foliation is a penetrative disjunctive cleavage with smooth and parallel cleavage domains. The minor presence of syn-kinematic sillimanite and the increase in the modal amount of white mica could indicate both a lower temperature of deformation and/or a higher amount of aqueous fluids available during shearing, with respect to the conditions of protomylonite (Carosi *et al.*, 2016a; Carosi *et al.*, 2016b).
The main deformation mechanism in quartz is grain boundary migration (Carosi *et al.*, 2016a) with only local incipient subgrain rotation recrystallization (Piazolo & Passchier, 2002; Stipp *et al.*, 2002; Passchier & Trouw, 2005). Feldspars are never fractured and show undulose extinction.
In this portion of the FMSZ the mylonitic foliation strikes N140-160 and steeply dips towards the NE. The mineral lineation plunges at low angle toward the NW. At the outcrop scale asymmetric and stretched leucosomes are recognizable. In thin section porphyroclasts with asimmetric strain shadows, mica fish, C' shear band are present. Kinematic indicators point to a top-to-the SW sense of shear.
Kinematic vorticity analysis point out to the presence of a general flow dominated by a component of pure shear but with a higher component of simple shear (Fig. 8a,b) with respect to the protomylonites (Carosi *et al.*, 2016b). θ angle are indicative of a transpressional deformation (Fig. 9) (Simonetti *et al.*, 2017).
In these outcrops it is also possible to observe post-mylonitic gentle folds with sub-horizontal axial planes affecting the mylonitic foliation (Fig. 10b). The folds occur also in the other lithotypes and are responsible of variations of the orientation of the mylonitic foliation. They are not associated to a ductile pervasive axial plane foliation and they have been related to a post-shearing tectonic collapse as they are compatible with a nearly vertical shortening direction.
We can then proceed along the GTA path and we reach the Passo delle Scolettas (2223 m) where other mylonitic gneiss crops out.

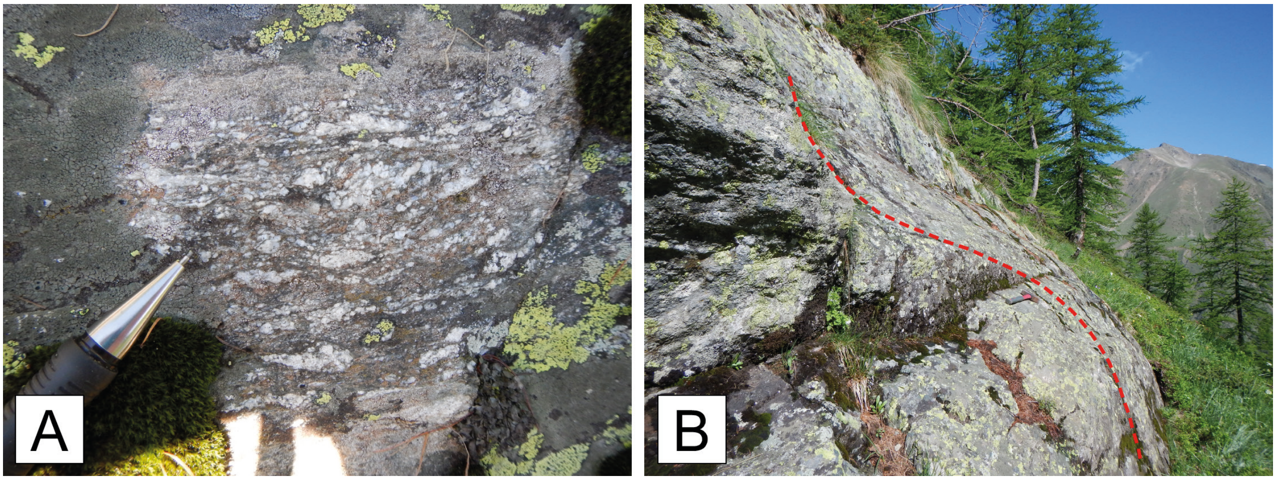

Fig. 10 - A) mylonites with sheared leucosomes and K-feldspar, plagioclase and quartz porphyloclasts in a fine grained biotite and white mica matrix; B) gentle folds with sub-horizontal axial planes affecting the mylonitic foliation.

Stop 4. Alpine shear zone (Coord. 44°18'36.18"N; 6°59'42.25"E)

From the Passo delle Scolettas we can take a nearly N-S small path which leads at the top of the Costabella del Piz (Fig. 5). Along the crest of the Costabella del Piz at about 2250 meters in height fine grained green mylonitic schist is present (Fig. 11a).

These mylonites are made up of quartz and feldspar porphyroclasts in a fine grained chlorite- and white mica-bearing matrix. The amount of fine grained matrix in this lithotype is about 65%-75%. Foliation strikes nearly E-W and dips at moderate to low angles toward the north with a north plunging mineral lineation (Fig. 11b). This Alpine mylonitic belt cross-cuts at low angle the mylonitic foliation of the FMSZ (Fig. 11c). S-C-C' fabric is indicative of reverse top-to-the S or SE sense of shear (Fig. 11f). In thin section it is possible to see that often shear bands deform an older higher temperature foliation with biotite relicts (Fig. 11f). Quartz deforms by subgrain rotation recrystallization (Piazolo & Passchier, 2002; Stipp *et al.*, 2002; Passchier & Trouw, 2005), feldspar porphyroclasts show undulose extinction and mechanical twins (Simpson & De Paor, 2008) and often they are fractured (Carosi *et al.*, 2016a). Several shear zones with the same features cross-cutting the FMSZ mylonitic foliation and the migmatitic foliation have been identified. These shear zones show differences in both thickness and lateral continuity but are all developed during greenschist facies metamorphism and are in agreement with a nearly N-S shortening. The most important of these belts is the one that crops out near the Colle Panieris, at the bottom of Monte Peiron, responsibile of the thrusting of basement rocks over the sedimentary cover of the Argentera Massif (Fig. 11d,e).

The Argentera Massif was involved in the Alpine orogeny at ~22 Ma (Corsini *et al.*, 2004; Sanchez *et al.*, 2011) but most of the Alpine deformation is concentrated in the sedimentary covers, detached from the metamorphic basement along evaporites and limestone breccias levels, in which several folding phases are recognizable (Barale *et al.*, 2016; d'Atri *et al.*, 2016). These shear zones, developed during greenschists-facies metamorphism, are the evidence of Alpine deformation in the basement during the lower Miocene (Carosi *et al.*, 2016a; Carosi *et al.*, 2016b; Baietto *et al.*, 2009). As the mylonitic bands are compatible from both a kinematic and metamorphic point of view with the two main alpine faults of the Argentera Massif, the strike slip Bersezio Fault-Zone and the reverse Fremamorta-Colle del Sabbione shear zone (Fig. 2, Baietto *et al.*, 2009), they can be interpreted as minor structures developed during the same regional Alpine deformation.

Stop 5. Mylonitic schists of the Ferriere-Mollières shear zone (Coord. 44°18'44.13"N; 6°59'39.52"E)

Proceeding along the crest toward the top of the Costabella del Piz (Fig. 5) shortly after the alpine shear zone, it is possible to observe the most classic mylonites of the Ferriere-Mollières shear zone (Fig. 12a).

Medium grained dark-green mylonitic schist made up of quartz, K-feldspar and plagioclase porphyroclasts in a fine grained biotite and white mica matrix (Fig. 12b). Sometimes garnet porphyroclasts are present. The amount of matrix is nearly 75%. The mylonitic schists are often associated with ultramylonitic bands (Uml) with a high amount of matrix (> 90 %) and very fine grainsize (Stop 6).

Foliation is a penetrative disjunctive cleavage with

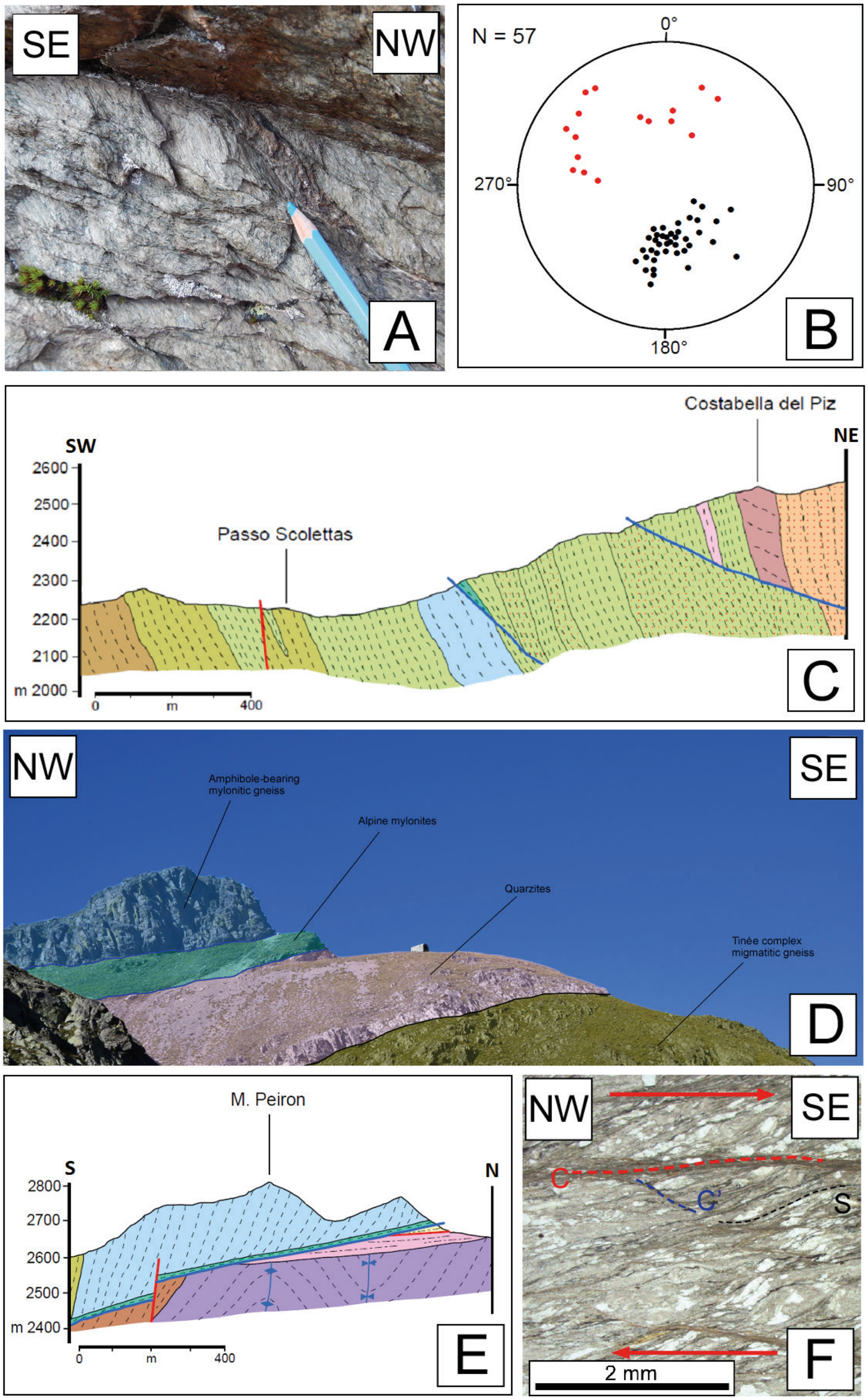

Fig. 11 - A) fine grained green mylonitic schist along the crest of the Costabella del Piz; B) lineation (red dots, 16 data) and poles to mylonitic foliation (black dots, 41 data) in the alpine shear zones; C) cross-section (section A, figure 3) along the crest of the Costabella del Piz (Carosi *et al.*, 2016a). Legend is the same as in figure 3. Alpine shear zone cross-cutting the mylonitic foliation of the FMSZ are in blue; D) Alpine mylonitic belt, delimited by blue lines, located near the Colle Panieris and M. Peiron (modified after Carosi *et al.*, 2016a); E) cross-section (section C', figure 3) showing basement rocks thrusted over the sedimentary cover of the Argentera Massif (modified after Carosi *et al.*, 2016a). Legend is the same as in figure 3; F) S-C-C' fabric showing a top-to-the SE sense of shear (parallel nicols). Along the S and C planes biotite relicts are present.

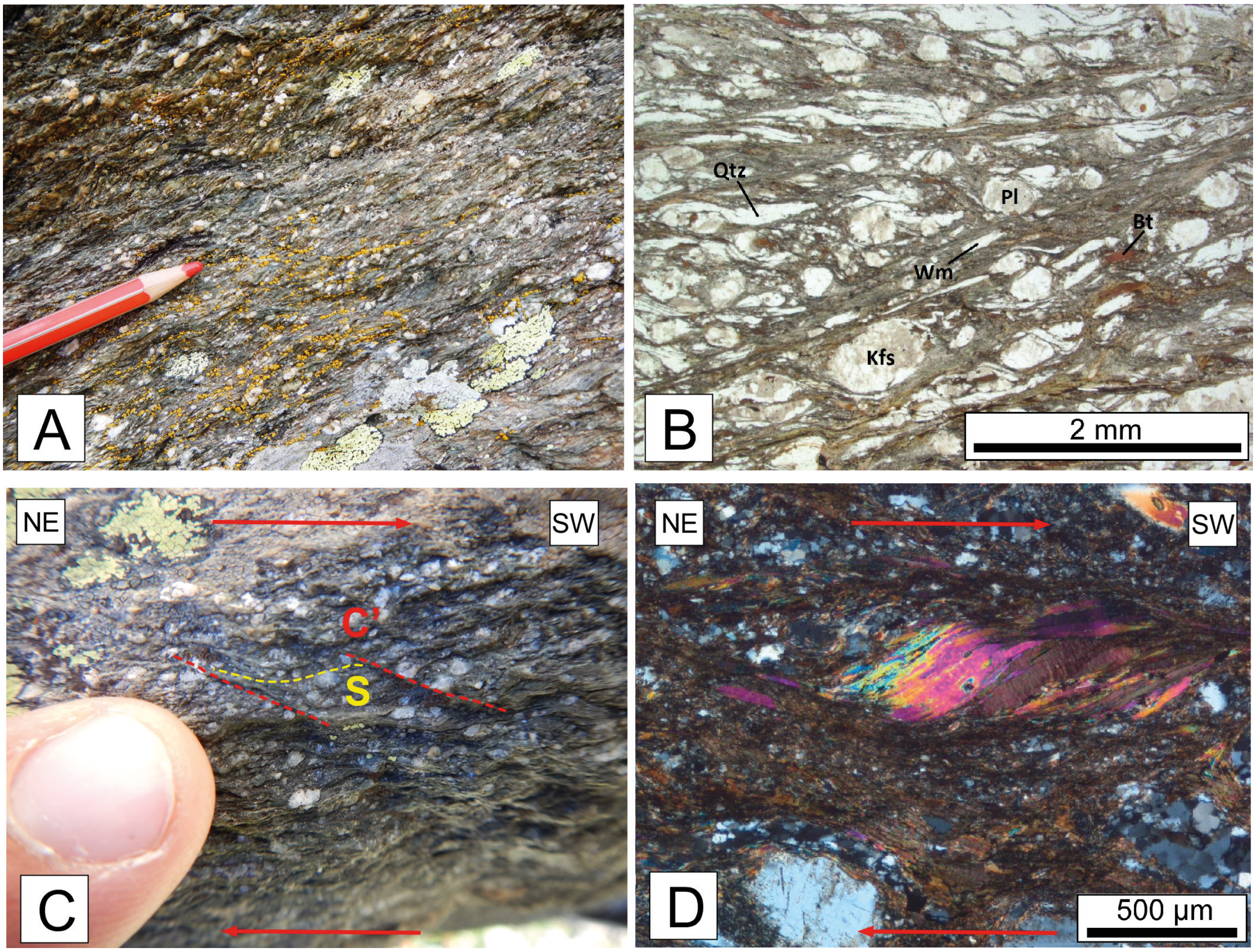

Fig. 12 - A) medium grained dark-green mylonitic schist of the FMSZ; B) appearance of the mylonites in thin section, quartz, K-feldspar and plagioclase porphyroclasts in a fine grained biotite and white mica matrix are recognizable (parallel nicols); C) S-C' fabric at the outcrop-scale pointing to a top-to-the SW sense of shear; D) foliation fish indicative of top-to-the SW sense of shear (crossed nicols).

smooth and parallel cleavage domain, it strikes NW-SE and steeply-dips toward the NE. A mineral lineation is present and plunges at low-angle toward the NW.

The biotite + white mica mineral assemblage (Fig. 12b) on the mylonitic foliation indicates an initial activation of the shear zone under amphibolite facies metamorphic conditions (Carosi *et al.*, 2016a; Carosi *et al.*, 2016b; Simonetti *et al.*, 2017). The absence of sillimanite on the shear planes is indicative of minor temperature of deformation with respect to the mylonitic gneiss and protomylonites cropping out at the margin of the shear zone.

Both at the outcrop-scale and in thin section it is possibile to recognize kinematic indicators showing a top-to-the SW sense of shear (Fig. 12c,d).

Kinematic vorticity analysis highlighted a general flow with a dominant component of pure shear and a subordinate component of simple shear (Fig. 8a,b) in agreement with the data collected in the other type of mylonites. The component of simple shear is higher with respect to the other mylonites of the FMSZ (Carosi *et al.*, 2016b). θ angle are indicative of a transpressive deformation (Fig. 9) (Simonetti *et al.*, 2017).

U-Th-Pb datings on syn-kinematic monazites constrain the age of shearing at ~320 Ma (Simonetti, 2015; Simonetti *et al.*, 2017), about 20 Ma younger with respect to the deformation recorded by the protomylonites (Stop 2).

Stop 6. Ultramylonites of the Ferriere-Mollières shear zone (Coord. 44°19'0.48"N; 6°59'46.54"E)

In the last stop of the field trip we can observe the most sheared rocks of the FMSZ that crop out along the crest of the Costabella del Piz (Fig. 5) at an altitude of 2400 m (Fig. 13a).

They are ultramylonites with an amount of matrix

over 90%. Foliation is a continuous cleavage (Fig. 13b) striking NW-SE and steeply dipping toward the NW. The attitude of the foliation is concordant with the mylonitic foliation in the FMSZ. Foliation is marked by white mica and chlorite (Fig. 11b). This mineral assemblage is indicative of a greenschist facies metamorphism. In agreement with the metamorphic conditions, quartz is mainly deformed by subgrain rotation recrystallization mechanism (Fig. 13c,d) (Piazolo & Passchier, 2002; Stipp *et al*., 2002; Passchier & Trouw, 2005) and the few feldspar porphyroclasts are fractured (Carosi *et al*., 2016b; Carosi *et al*., 2016a).
Kinematic indicators point to a dextral top-to-the SW sense of shear (Fig. 13d).
Flow analysis in the ultramylonites (Fig. 8b) highlighted a general shear with a prevalent component of simple shear (Carosi *et al*., 2016b). θ angles are indicative of a simple shear-dominated transpression (Fig. 9).

Discussion

Recent detailed structural-geological mapping combined with detailed structural and petrographical analysis (Simonetti, 2015; Carosi *et al*., 2016a) allowed the identification and mapping of different types of mylonites within the FMSZ and revealed the presence of greenschist-facies Alpine shear zones cross-cutting variscan foliations.
Kinematic vorticity analysis carried out by Simonetti (2015), Carosi *et al*. (2016b) and Simonetti *et al*. (2017) highlighted a deformation regime compatible with an heterogeneous transpressional setting with variation in the percentage of pure shear and simple shear (Fossen *et al*., 1994). In addition the attitude of the mylonitic foliation is sub-vertical along the ~20 km length of the shear zone, in agreement with a transpressive setting (Fossen *et al*., 2004).
In the case of transtensional deformation as suggested

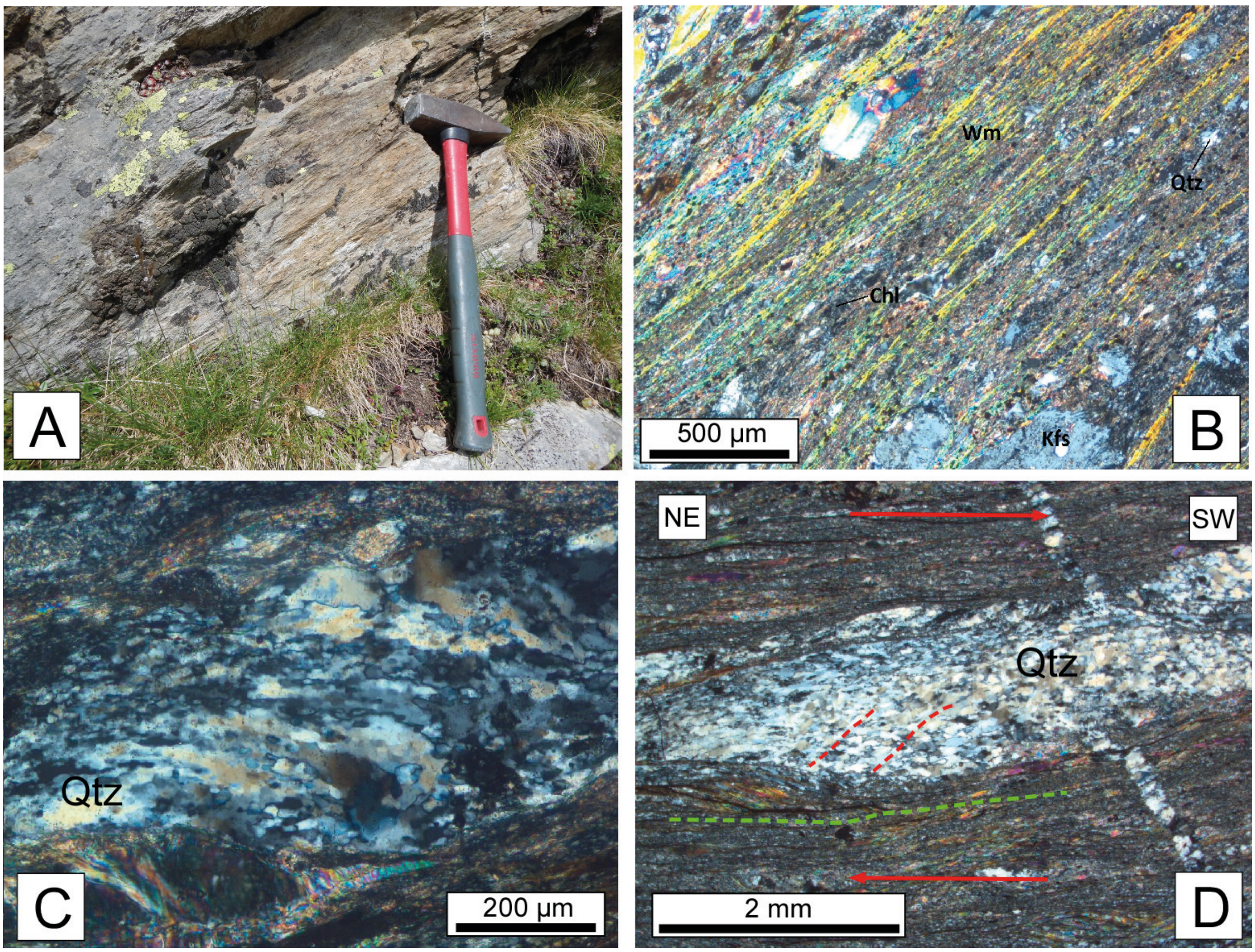

Fig. 13 - A) ultramylonites along the crest of the Costabella del Piz; B) continuous cleavage marked by white mica and chlorite; C) quartz deformed by subgrain rotation recrystallization; D) stretched quartz domain deformed by subgrain rotation and recrystallization showing an oblique foliation (marked in red) pointing to a top-to-the SW sense of shear.

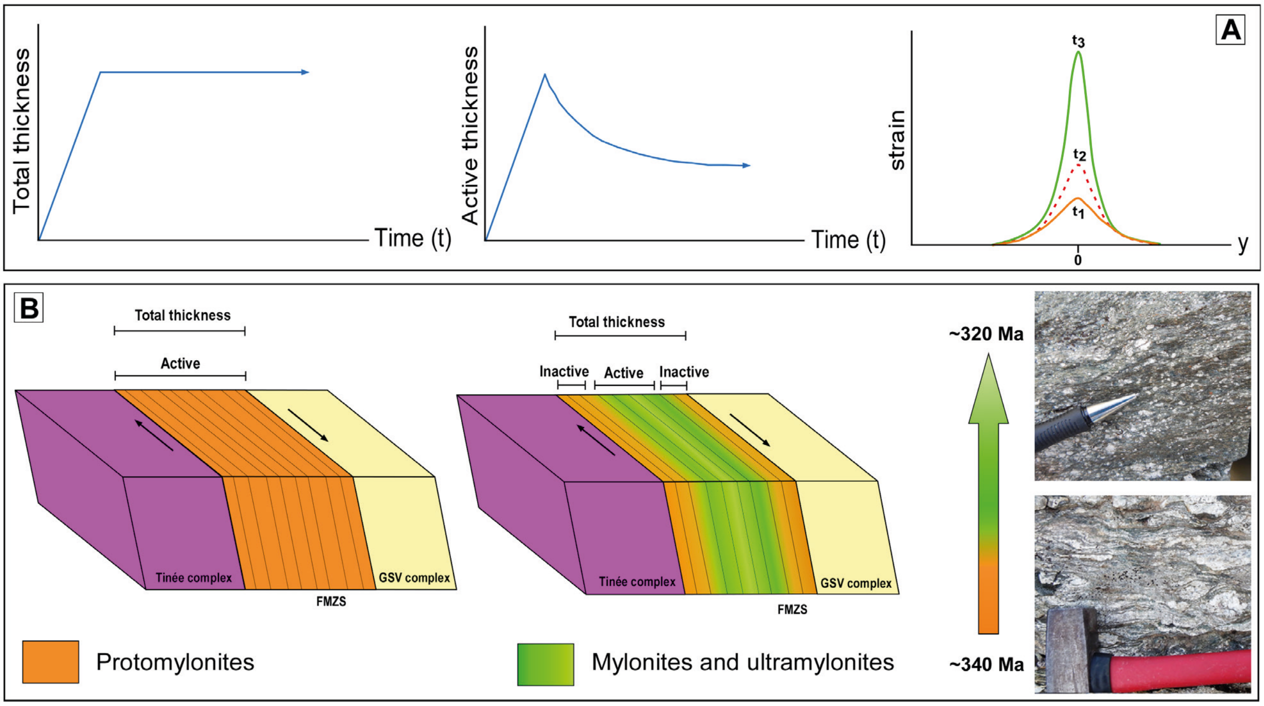

Fig. 14 - A) growth of a type II shear zone: graphs show the relationship between the total thickness and the active thickness during time and the amount of strain within the shear zone. With time the deformation is concentrated in the central part of the shear zone and the margins become inactive. Because of this the active thickness progressively decrease while the total thickness remains constant; B) Evolution of the Ferriere-Molliéres Shear Zone according to a type II growth-model and relationship between deformation gradient and age of the shear (Carosi *et al.*, 2016b). The two photographs show the aspect of protomylonites ad mylonites at the outcrop scale. It is possible to note the larger grain size and the presence of sheared leucosomes in the protomylonites whereas mylonites are subjected to a strong grain size reduction and a larger amount of matrix is present.

by Musumeci & Colombo (2002) the attitude of mylonitic foliation is expected to be sub-horizontal due to the main sub-vertical shortening direction (Fossen *et al.*, 1994).

The presence of medium to high-grade metamorphic mylonites associated with lower-grade ones, localized in the central part of the FMSZ, the strong deformation gradient, the difference in the deformation regime and the different age of deformation allow us to interpret the FMSZ as a strain softening type-II shear zone (Fossen, 2010). In this kind of shear zones deformation progressively concentrates in the central part because of strain softening (due to the presence of channeled fluids, metamorphic reactions and grain size reduction) living the external parts of the structure inactive (Fig. 14a).

Differently from what has been proposed by Sanchez *et al.* (2011), the FMSZ is a still preserved Variscan transpressive shear zone. FMSZ is also a good example of strain softening regional-scale shear zone (Carosi *et al.*, 2016b; Simonetti *et al.*, 2017) which evolves during decreasing temperature conditions: in the external parts of the FMSZ features acquired during the early stage of shear deformation are preserved while the internal part records features of the final stage of activity of the shear zone (Fig. 14b).

Data obteined in the FMSZ also contribute to reinforce the model proposed by Rollet *et al.* (2002), Rosenbaum *et al.* (2002) and Advokaat *et al.* (2014) where the Corsica-Sardinia Block is connected to southern France and it is in continuity with Western Alps as all these fragments of the Variscan Belt show similarities from both the lithological and the structural point of view (Carosi & Palmeri, 2002; Corsini & Rolland, 2009; Carosi *et al.*, 2012; Simonetti *et al.*, 2017).

Conclusive Remarks

In this field trip we presented key outcrops where the different types of mylonites within the FMSZ and the main features of the shear zone can be observed. Summing, these observations suggest that:

- Alpine greenschist-facies deformation is localized in ductile top-to-the SSE shear zones that cross-cut variscan structural elements;

- A deformation gradient is recognizable from the marginal part of the FMSZ shear zone toward the central part. Along this gradient a transition from protomylonites to mylonites and ultramylonites is detectable;
- Foliation and mineral lineation of the FMSZ, in the different type of mylonites, always show a constant trend of orientation. Axial plane of the folds in the GSV complex and Tinèe complex is sub-parallel to the mylonitic foliation;
- Deformation develops during retrograde metamorphic conditions from high-temperature amphibolite-facies to greenschist-facies. Deformation temperature within the FMSZ decreases along the deformation gradient. In particular the protomylonites are characterized by the presence of syn-kinematic sillimanite along C and C' planes that are indicative of a high temperature of deformation (HT amphibolite-facies conditions). In the mylonites the growth of syn-kinematic white mica and biotite is indicative of a lower temperature of deformation (LT amphibolite-facies conditions). These observations are also supported by the variation of the deformation mechanisms of quartz;
- Along the deformation gradient of the FMSZ a variation in the deformation regime from a pure shear-dominated transpression to a simple shear-dominated transpression can be observed;
- The age of the shear deformation is progressively younger along the deformation gradient. The FMSZ shows a nearly 20 Ma long lasting deformation history.

ACKNOWLEDGEMENTS

The field trip has been realized in the Argentera Massif during summer 2015 as part of three master theses by Simonetti (Università di Torino), Mammoliti (Università di Pisa) and D'Addario (Università di Pisa). We thank two anonymous reviewers for their careful revisions that significantly improved the quality of the manuscript.

REFERENCES

Advokaat E.L., van Hinsbergen D.J.J., Maffione M., Langereis C.G., Vissers R.L.M., Cherchi A., Schroeder R., Madani H., Columbu S., 2014. Eocene rotation of Sardinia, and the paleogeography of the western Mediterranean region. *Earth and Planetary Science Letters* 401: 183-195.

Arthaud F., Matte P., 1977. Late Paleozoic strikeslip faulting in southern Europe and northern Africa; result of a right-lateral shear zone between the Appalachians and the Urals. *Geological Society of America Bulletin* 88: 1305-1320.

D'Atri A., Piana F., Barale L., Bertok C., Martire L., 2016. Geological setting of the southern termination of Western Alps. *International Journal of Earth Sciences* 105: 1831-1858.

Baietto A., Perello P., Cadoppi P., Martinotti G., 2009. Alpine tectonic evolution and thermal water circulations of the Argentera Massif (South-Western Alps). *Swiss Journal of Geosciences* 102: 223-245.

Barale L., Bertok C., d'Atri A., Martire L., Piana F., Domini G., 2016. Geology of the Entracque-Colle di Tenda area (Maritime Alps, NW Italy). *Journal of Maps* 12: 359-370.

Burg J.-P., Matte P., 1978. A cross section through the French Massif Central and the scope of its Variscan Geodynamic Evolution. *Zeitschrift der Deutschen Geologischen Gesellschaf* 129: 429-460.

Carmignani L., Carosi R., Anselmo D.P., Gattiglio M., Musumeci G., Oggiano G., Pertusati P.C., 1994. The hercynian chain in Sardinia (Italy) La chaîne hercynienne de Sardaigne (Italie). *Geodinamica Acta* 7: 31-47.

Carosi R., D'Addario E., Mammoliti E., Montomoli C., Simonetti M., 2016a. Geology of the northwestern portion of the Ferriere-Mollieres Shear Zone, Argentera Massif, Italy. *Journal of Maps* 12: 466-475.

Carosi R., D'Addario E., Mammoliti E., Montomoli C., Simonetti M., 2016b. Vorticty of the flow and strain analysis in the Argentera Massif (External Crystalline Massifs, Western Alps): recognition of a regional pure-shear dominated transpression. *Rendiconti Online Società Geologica Italiana* 40: 165.

Carosi R., Montomoli C., Iaccarino S., Massonne H.-J., Rubatto D., Langone A., Geminiani L., Visonà D., 2016c. Middle to late Eocene exhumation of the Greater Himalayan Sequence in the Central Himalayas: Progressive accretion from the Indian plate. *Geological Society of America Bulletin* 128(11-12): 1571-1592.

Carosi R., Frassi C., Montomoli C., 2009. Deformation during exhumation of medium- and high-grade metamorphic rocks in the Variscan chain in northern Sardinia (Italy). *Geological Journal* 44: 280-305.

Carosi R., Montomoli C., Tiepolo M., Frassi C., 2012. Geochronological constraints on post-collisional shear zones in the Variscides of Sardinia (Italy): Post-collisional shear zones in the Variscides of Sardinia. *Terra Nova* 24: 42-51.

Carosi R., Palmeri R., 2002. Orogen-parallel tectonic transport in the Variscan belt of northeastern Sardinia (Italy): implications for the exhumation of medium-pressure metamorphic rocks. *Geological Magazine* 139: 497-511.

Compagnoni R., Ferrando S., Lombardo B., Radulesco N., Rubatto D., 2010. Paleo-European crust of the Italian Western Alps: Geological history of the Argentera Massif and comparison with Mont Blanc-Aiguilles Rouges and Maures-Tanneron Massifs. *Journal of the Virtual Explorer* 36: paper 3.

Compagnoni R., Lombardo B., Prato R., 1974. Andalousite et sillimanite aux contacts du granite central de l'Argentera (Alpes Maritimes). *Rendiconti della Società Italiana di Mineralogia e Petrologia* 30: 31-54.

Corsini M., Ruffet G., Caby R., 2004. Alpine and late-hercynian geochronological constraints in the Argentera Massif (Western Alps). *Eclogae Geologicae Helvetiae* 97: 3-15.

Corsini M., Rolland Y., 2009. Late evolution of the southern European Variscan belt: exhumation of the lower crust in a context of oblique convergence. *Comptes Rendus Geosciences* 341(2-3): 214-223.

Dewey, J.F., Holdsworth, R.E., Strachan, R.A., 1998. Transpression and transtension zones. Geological Society, London, Special Publications 135: 1-14.

Di Vincenzo G., Carosi R., Palmeri R., 2004. The Relationship between Tectono-metamorphic Evolution and Argon Isotope Records in White Mica: Constraints from in situ 40Ar-39Ar Laser Analysis of the Variscan Basement of Sardinia. *Journal of Petrology* 45: 1013-1043.

Faure-Muret A., 1955. Etudes géologiques sur le massif de l'Argentera-Mercantour et ses enveloppes sédimentaires. Unpublished PhD dissertation, Paris, 336 pp.

Ferrando S., Lombardo B., Compagnoni R., 2008. Metamorphic history of HP mafic granulites from the Gesso-Stura Terrain (Argentera Massif, Western Alps, Italy). *European Journal of Mineralogy* 20: 777-790.

Ferrara G., Malaroda R., 1969. Radiometric age of granitic rocks from the Argentera Massif (Maritime Alps). *Bollettino della Società Geologica Italiana* 88: 311-320.

Fossen H., 2010. Structural geology. Cambridge University Press, Cambridge; New York.

Fossen H., Tikoff B., 1993. The deformation matrix for simultaneous simple shearing, pure shearing and volume change, and its application to transpression-transtension tectonics. *Journal of Structural Geology* 15: 413-422.

Fossen H., Tikoff B., Teyssier C., 1994. Strain modeling of transpressional and transtensional deformation. Norsk Geologisk Tidsskrift 74: 134-145.

Fossen H., Cavalcante G. C. G., 2017. Shear zones – A review. *Earth-Science Reviews* 171: 434-455.

Franke W., 1989. Tectonostratigraphic units in the Variscan belt of central Europe. In: Dallmeyer, R. D. (ed.) Terranes in the Circum-Atlantic Paleozoic Orogens. *Geological Society of America Special Paper* 230: 67-90.

Gerbault M., Schneider J., Reverso-Peila A., Corsini M., 2016. Crustal exhumation during ongoing compression in the Variscan Maures-Tanneron Massif, France-Geological and thermo-mechanical aspects. *Tectonophysics* doi: 10.1016/j.tecto.2016.12.019.

Gillam B.G., Little T.A., Smith E., Toy V.G., 2013. Extensional shear band development on the outer margin of the Alpine mylonite zone, Tatare Stream, Southern Alps, New Zealand. *Journal of Structural Geology* 54: 1-20.

Goscombe B. D., Grey D. R., 2009. Metamorphic response in orogens of different obliquity, scale and geometry. *Gondwana Reserch* 15, 2: 151-167.

Horner F., Lowrie W., 1981. Paleomagnetic evidence from Mesozoic carbonate rocks for the rotation of Sardinia. *Journal of Geophysical Research* 49(1): 11-19.

Iaccarino S., Montomoli C., Carosi R., Massonne H.-J., Langone A., Visonà D., 2015. Pressure-temperature-time deformation path of kyanite-bearing migmatitic paragneiss in the Kali Gandaki valley (Central Nepal): Investigation of Late Eocene-Early Oligocene melting processes. *Lithos* 231: 103-121.

Iaccarino S., Montomoli C., Carosi R., Massonne H.-J., Visonà D., 2017, Geology and tectono-metamorphic evolution of the Himalayan metamorphic core: insights from the Mugu Karnali transect, Western Nepal (Central Himalaya). *Journal of Metamorphic Geology* 35, 3: 301-325.

Iacopini D., Frassi C., Carosi R., Montomoli C., 2011. Biases in three-dimensional vorticity analysis using porphyroclast system: limits and application to natural examples: Geological Society, London, Special Publications 360: 301-318.

Jessup M.J., Law R.D., Frassi C., 2007. The Rigid Grain Net (RGN): An alternative method for estimating mean kinematic vorticity number (Wm). *Journal of Structural Geology* 29: 411-421.

Kohn M.J., Wieland M., Parkinson C.D., Upreti B.N., 2004, Miocene faulting at plate tectonic velocity in the Main Central thrust region, central Nepal. *Earth and Planetary Science Letters* 228: 299-310.

Kurz G.A., Northrup C.J., 2008. Structural analysis of mylonitic rocks in the Cougar Creek Complex, Oregon–Idaho using the porphyroclast hyperbolic distribution method, and potential use of SC′-type extensional shear bands as quantitative vorticity indicators. *Journal of Structural Geology* 30: 1005-1012.

Law R.D., Searle M.P., Simpson R.L., 2004. Strain, deformation temperatures and vorticity of flow at the top of the Greater Himalayan Slab, Everest Massif, Tibet. *Journal of the Geological Society* 161: 305-320.

Malaroda R., Carraro F., Dal Piaz G.V., Franceschetti B., Sturani C., Zanella E., 1970. Carta geologica del Massiccio dell'Argentera alla scala 1:50.000 e note illustrative. *Memorie della Società Geologica Italiana* 9: 557-663.

Matte P., 1986. La Chaîne varisque parmi les chaînes paléozoïques péri-atlantiques, modèle d'évolution et position des grands blocs continentaux au Permo-Carbonifère. *Bulletin de la Société géologique de France* 8: 4-24.

Montomoli C., Iaccarino S., Carosi R., Langone A., Visonà D., 2013. Tectonometamorphic discontinuities within the Greater Himalayan Sequence in Western Nepal (Central Himalaya): Insights on the exhumation of crystalline rocks. *Tectonophysics* 608: 1349-1370.

Musumeci G., Colombo F., 2002. Late Visean mylonitic granitoids in the Argentera Massif (Western Alps): age and kinematic constraints on the Ferrière-Mollières shear zone. *Comptes Rendus de l'Académie des Sciences Serie II* 334: 213-220.

Oliot E., Melleton J., Schneider J., Corsini M., Gardie, V., Rolland Y., 2015. Variscan crustal thickening in the Maures-Tanneron massif (South Variscan belt, France): new in situ monazite U-Th-Pb chemical dating of high-grade rocks. *Bulletin de la Société géologique de France* 186: 145-169.

Passchier C.W., 1987. Stable position of rigid objects in non-coaxial flow: a study in vorticity analysis. *Journal of Structural Geology* 9: 679-690.

Passchier C.W., 1991. The classification of dilatant flow type. *Journal of Structural Geology* 13: 101-104.

Passchier C.W., Trouw R.A.J., 2005. Microtectonics. Springer, Berlin. 366 pp.

Piazolo S., Passchier C. W., 2002. experimental modelling of viscous inclusions in a circular high-strain ring: implication for the interpretation of shape fabrics and deformed enclaves. *Journal of Geophysical Research* 107, B10, 2242, ETG 11. 1-15.

von Raumer J.F., Bussy F., Stampfli G.M., 2009. The Variscan evolution in the External massifs of the Alps and place in their Variscan framework. *Comptes Rendus Geoscience* 341: 239-252.

Rollet N., Déverchère J., Beslier M.-O., Guennoc P., Réhault J.-P., Sosson M., Truffert C., 2002. Back arc extension, tectonic inheritance, and volcanism in the Ligurian Sea, Western Mediterranean: Ligurian sea back arc structure and evolution. *Tectonics* 21: 6-1-6-23.

Rosenbaum G., Lister G.S., Duboz C., 2002. Reconstruction of the tectonic evolution of the western Mediterranean since the Oligocene. *Journal of the Virtual Explorer* 08.

Rubatto D., Schaltegger U., Lombardo D., Colombo F., Compagnoni R., 2001. Complex Paleozoic magmatic and metamorphic evolution in the Argentera massif (Western Alps), resolved with U-Pb dating. *Schweizerische mineralogische und petrographische Mitteilungen* 81: 213-228.

Rubatto D., Ferrando S., Compagnoni R., Lombardo B., 2010. Carboniferous high-pressure metamorphism of Ordovician protoliths in the Argentera Massif (Italy), Southern European Variscan belt. *Lithos* 116(1-2): 65-76.

Sanchez G., Rolland Y., Schneider J., Corsini M., Oliot E., Goncalves P., Verati C., Lardeaux J.-M., Marquer D., 2011. Dating low-temperature deformation by 40Ar/39Ar on white mica, insights from the Argentera-Mercantour Massif (SW Alps). *Lithos* 125: 521-536.

Schneider J., Corsini M., Reverso-Peila A., Lardeaux J.-M., 2014. Thermal and mechanical evolution of an orogenic wedge during Variscan collision: an example in the Maures-Tanneron Massif (SE France). *Geological Society, London, Special Publications* 405: 313-331.

Sibson R.H., 1977. Fault rocks and fault mechanisms. *Journal of the Geological Society* 133: 191-213.

Simonetti M., 2015. La 'Ferriere - Mollieres Shear Zone' (Massiccio dell' Argentera, Alpi Occidentali): rilevamento geologico, analisi strutturale e cinematica del flusso nella zona del Vallone di Pontebernardo (Pietraporzio, CN). Unpublished PhD dissertation, Università degli Studi di Torino (Italy), 182 pp.

Simonetti M., Carosi R., Montomoli C., Langone A., 2017. Geochronology and deformation in the Ferriere- Mollières shear zone (Argentera Massif, Western Alps): similarities and differences compared to other fragments of the Variscan Chain in the Mediterranean area. *Geosciences: a tool in a changing world, SGI abstract book,* doi: 10.3301/ABSGI.2017.01.

Simpson C., De Paor D., 2008. An atlas of deformation microstructures with selected animations. *Journal of the Virtual Explorer* 31: paper 2.

Stampfli G.M., Borel G.D., Marchant R., Mosar J., 2002. Western Alps geological constraints on western Tethyan reconstructions. *Journal of the Virtual Explorer* 08.

Stipp M., Stunitz H., Heilbronner R., Schmid S. M., 2002. The eastern Tonale fault zone: a "natural laboratory" for crystal plastic deformation of quartz over a temperature range from 250 to 700° C. *Journal of Structural Geology* 24: 1861-1884.

Tollmann A., 1982. Großraumiger variszischer Deckenbau im Moldanubikum und neue Gedanken zum Variszikum Europas. *Geotektonische Forschungen* 64: 1-91.

Thompson A. B., Schulmann K., Jezek J., 1997, Thermal evolution and exhumation in obliquely convergent (transpressive) orogens. *Tectonophysics* 280: 171-184.

Wallis S.R., Platt J.P., Knott, S.D., 1993. Recognition of syn-convergence extension in accretionary wedges with examples from Calabrian arc and the Eastern Alps. *American Journal of Sciences* 293: 463-495.

Xypolias P., 2010. Vorticity analysis in shear zones: a review of methods and applications. *Journal of Structural Geology* 32: 2072-2092.

(ms. pres. 07 luglio 2017; ult. bozze 03 novembre 2017)

Edizioni ETS
Piazza Carrara, 16-19, I-56126 Pisa
info@edizioniets.com - www.edizioniets.com
Finito di stampare nel mese di dicembre 2017